Hindawi
Wireless Communications and Mobile Computing
Volume 2021, Article ID 6639894, 12 pages
https://doi.org/10.1155/2021/6639894

Research Article

A Novel Subcarrier-Level Spectrum Sensing Method by Utilizing Fine-Grained Channel State Information in Wireless Networks

Zheng Lu[1,2] **Handong Wang**,[1,2] **Hongyu Sun**[1,2] **Chin-Ling Chen**,[3,4,5] **and Zhenjiang Tan**[1,2]

[1]*Department of Computer Science, Jilin Normal University, Siping 136000, China*
[2]*State Key Laboratory of Numerical Simulation, Jilin Province, Siping 136000, China*
[3]*Department of Computer Science and Information Engineering, Chaoyang University of Technology, Taizhong 41349, Taiwan*
[4]*School of Information Engineering, Changchun Sci-Tech University, Changchun 130000, China*
[5]*School of Computer and Information Engineering, Xiamen University of Technology, Xiamen 360000, China*

Correspondence should be addressed to Chin-Ling Chen; clc@mail.cyut.edu.tw and Zhenjiang Tan; tanzj@jlnu.edu.cn

Received 31 December 2020; Revised 23 February 2021; Accepted 12 March 2021; Published 7 May 2021

Academic Editor: Feng-Jang Hwang

Traditionally, the channelization structures of wireless technologies (802.11/ZigBee/BLE) have been fixed. Each node content for the spectrum is assigned one channel with a specific bandwidth. However, classical channel-based spectrum sensing and sharing algorithms have great limitations to further optimize spectrum utilization when multiple IoT with different wireless technologies coexisting in the same environment. Therefore, exploring the fine-grained spectrum sensing algorithm becomes an essential work to further improve the spectrum utilization efficiency, especially in the Industrial Scientific Medical (ISM) band. This paper proposes *Subcarrier-Sniffer*, a novel subcarrier-level spectrum sensing and sharing method, which utilizes channel state information (CSI) to sense the fine-grained status of each subcarrier of the traditional channel. To evaluate the performance of *Subcarrier-Sniffer*, we implemented *Subcarrier-Sniffer* by USRP B200min, and the experimental results show that the accuracy of subcarrier-level spectrum sensing could achieve 100% in our settings that the distance between *Subcarrier-Sniffer* and the monitor is not greater than 7 m. *Subcarrier-Sniffer* could be applied in WiFi and ZigBee, WiFi and BLE, and WiFi and LTE-U coexisted environments for better spectrum utilization.

1. Introduction

Most of the wireless technologies today operate with the default bandwidth, for example, the default bandwidth of 802.11n is 20 MHz, while the default bandwidths of ZigBee and BLE are 3 MHz and 2 MHz, respectively. However, the channels are partially overlapped in ISM 2.4 GHz which hampers further optimize the limited spectrum resource. Moreover, the ever-increasing of the heterogeneous IoT devices coexisting in interfered environments also motivated the developing spectrum sharing and management techniques [1]. The spectrum sensing and sharing algorithms are widely used in a variety of wireless technologies, for example, DeepWiFi [2] for WiFi spectrum sensing, OutSense [3] for ZigBee spectrum sensing, and RealSense [4] for TV spectrum sensing. Spectrum sensing and sharing methods are also used in cross-technology coexisted environments, for example, literature [5–11] conducts the spectrum sensing and management between WiFi and LTE-U technologies, literature [12–15] introduces the spectrum sensing between ZigBee and WiFi technologies, [16–21], uses spectrum sensing method for OFDM-based heterogeneous wireless devices.

However, most of the current work uses a channel-based spectrum sensing algorithm to share ISM band resources [22]. For example, WiFi defines 11 channels with 20 MHz bandwidth, ZigBee defines 26 channels with 3 MHz bandwidth, and Bluetooth 4.0 defines 30 channels with 2 MHz bandwidth in the 2.4 GHz ISM bands. Therefore, the channel bandwidths

of WiFi, ZigBee, and BLE are 20 MHz, 3 MHz, and 2 MHz, respectively. It is obvious that channel-based contention methods between heterogeneous wireless technologies deployed in the interfered environment could not further optimize spectrum utilization, Figure 1 illustrates the spectrum wasting between the narrow-wide band and wide-wide band technologies coexisting scenarios.

Figure 1(a) shows the disadvantage of channel-based spectrum sharing methods when narrow-wide band wireless technologies coexisted in the same interfered environment since both of them trying to access the idle channel which practically overlapped in the spectrum, and only one of them could obtain the channel. Suppose the bandwidth of the wideband technology is x MHz and the bandwidth of the narrowband technology is y. Thus, the wasted spectrum is $(x - y)$ MHz when the narrowband technology allocating the channel. Figure 1(b) shows the spectrum wasting when two different wideband technologies content the same channel, and assume that there n MHz of the subcarriers are idle in the first wideband technology, and m MHz subcarriers are idle in the second wideband technology. If the idle subcarriers are not overlapping, the total maximum spectrum wasting is $(m + n)$ MHz. Therefore, it is obvious that the subcarrier-level spectrum sensing and sharing method could further optimize the spectrum efficiency in ISM bands when massive heterogeneous wireless technologies are deployed in the same interfered environments.

Since the channel-level spectrum sensing methods determine whether the channel is idle by measuring the signal-to-noise ratio (SNR) changes (such as SNR and RSS) of the channel's frequency center, the subcarrier-level spectrum sensing methods measure fine-grained SNR in each subcarrier to determine the status of the fine-grained spectrum. Therefore, the design challenges introduced by the fine-grained subcarrier-level spectrum sensing and sharing methods are at least as follows: (i) how to perform energy-efficient subcarrier-level spectrum sensing algorithm without affecting normal communications. The traditional method uses full-spectrum scanning to sense the energy variation of each subcarrier, which affects normal communication and requires an expensive device with a relatively high sampling rate. To solve this challenge, this paper proposes to use channel state information (CSI) to sense the subcarrier-level SNR sensing, (ii) how to remove the noise jitters of each subcarrier caused by the frequency selective characteristics of the signal; therefore, for the wideband end, how to obtain the pure SNR jitters caused by the narrowband signal interference is a significant challenge; to solve this problem, this paper collects the initial state of CSI first to fetch the environmental information without cross-technology interference, and (iii) how to determine which subcarriers do have serious interference according to the SNR jitters generated by the interference is another design challenge of subcarrier-level spectrum sensing algorithm. The main reason for the problem is that if the narrowband signal is 3 MHz, the interference range (IR) caused by harmonics usually satisfies IR = $\alpha + 3 + \beta$MHz, where α and β are, respectively, the influence on the left and right spectrum range of 3 MHz. To solve this problem, a method for delimiting the range of interfered subcarriers is proposed.

Specifically, the contributions of this paper are detailed as follows:

(1) We first propose to use channel state information collected from the off-the-shelf wireless devices to evaluate the subcarrier interference and guide the spectrum sensing and sharing algorithm for optimized spectrum utilization

(2) We propose a denoise method base on the initial state of the CSI profile to recognize the narrowband utilization in a more precise way

(3) We propose a threshold-based interference range determination method to identify the interfered subcarriers when wideband and wideband coexist in the propagation scenarios

(4) We implemented the system using USRP B200min and analyze the performance of *Subcarrier-Sniffer*, and the experimental results show that the accuracy of *Subcarrier-Sniffer* could achieve 100% when the distance between *Subcarrier-Sniffer* and the monitor is not greater than 7 m

The rest of this paper is organized as follows: Section 2 introduces the related works, Section 3 introduces the theory of our method, Section 4 shows the evaluation results, and the conclusion is in Section 5.

2. Related Works

To further optimize the spectrum utilization in the ISM band, researchers have explored various nonchannel-based spectrum sensing and allocation methods. Subcarrier-Sniffer is closely related to three broad areas: (i) fine-grained channel access methods, (ii) adapted width channel access methods, and (iii) narrow-wide band coexistence methods.

2.1. Fine-Grained Channel Access Methods. FICA [23] splits a channel into multiple subchannels and allows devices content for subchannels, which could reduce the MAC-layer overhead of high-rate WLANs. It uses a frequency-domain back-off algorithm that cannot coexist directly with current 802.11 WLANs. Moreover, FICA requires a tight synchronization between all nodes contend for spectrum, which could not retain the distributed mechanism in CSMA/CA protocol. FSS [24] proposes a fine-grained spectrum sharing method for fair and efficient spectrum utilization between existed and emerging 802.11 protocols with various channel widths. It allows users to contend for each spectrum chunk and opportunistically split a wideband channel or bond multiple discontinuous chunks to ensure fair and efficient access to the available spectrum. The authors of [25] propose to divide a frame into multiple miniframes and divide the channel into multiple minichannels; they use a greedy spectrum assignment algorithm to determine where to place the miniframes, without considering the guard band cost of noncontiguous minichannels.

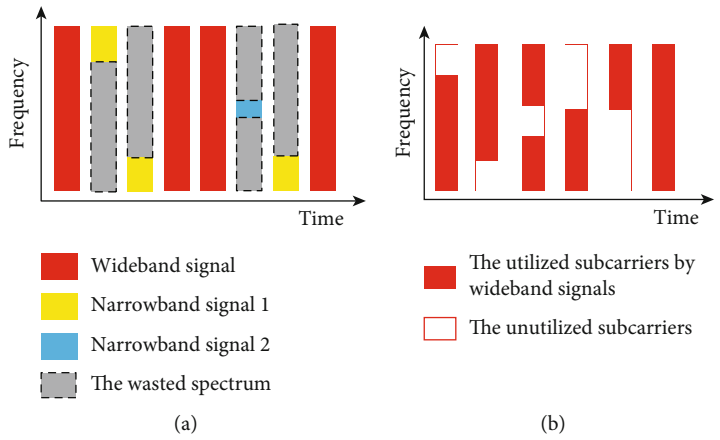

Figure 1: Spectrum wasting under channel-based sensing methods: (a) narrow-wide band technologies coexisting scenarios and (b) wide-wide band technologies coexisting scenarios.

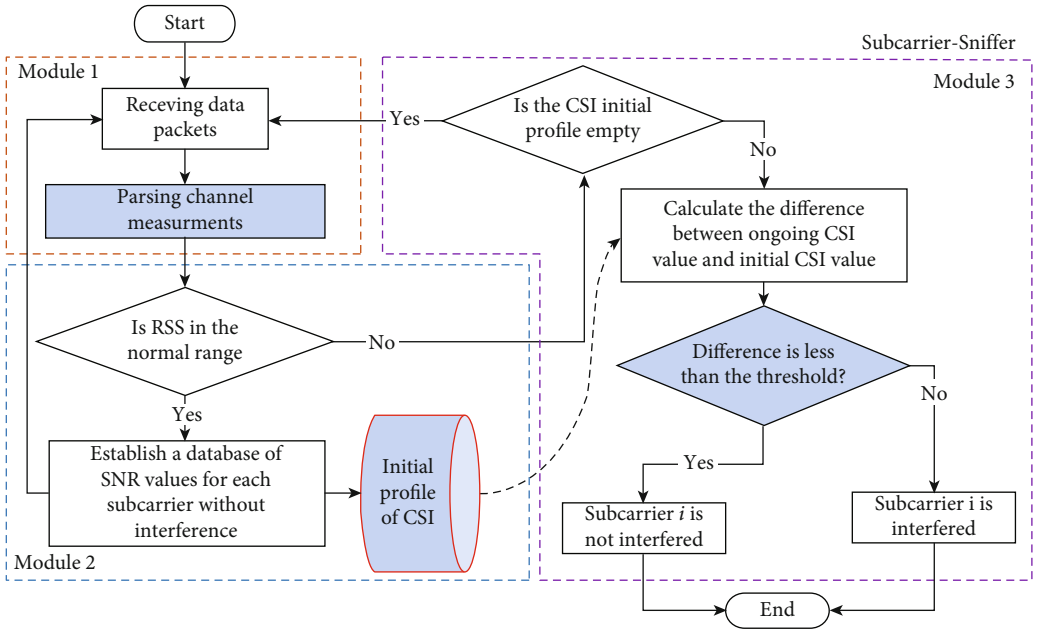

Figure 2: Design overview of Subcarrier-Sniffer.

2.2. Adaptable Width Channel Access Methods. The proposal of IEEE standards such as 802.11n [26] and 802.11ac [27] suggested changing channel width adaptively for spectrum utilization. FLUID [28] uses flexible channelization, which allows each transmitter to choose the appropriate channel width and center frequency for transmission. The experimental results show that flexible channelization can improve the throughput of the system. The authors of [29] modeled the adaptive width channel allocation from a game-theoretic point of view, in which the node is rational and always pursue their objectives. The authors of [30] explored the benefits of adapting channel width to balance the trade-off between through and energy efficiency. Article [31] proposes to share the spectrum according to throughput requirements and signal strength values of a specific node. [32] proposed to change both the frequency center and bandwidth to match network traffic loads.

2.3. Narrow-Wide Band Coexistence Methods. As the deployment of heterogeneous IoT devices in an indoor environment, researchers proposed several narrow-wide band coexistence methods to optimize spectrum utilization in ISM bands. SWIFT [32] proposes to enable the coexistence between the OFDM-based ultrawideband (UWB) system and the WiFi WLANs that have a relatively narrower bandwidth. LASI [11] enables simultaneous transmission between LTE and WiFi in ISM 5G bands by low-amplitude injection methods. B^2W^2 [14] designed N-way concurrent cross-technology communications while concurrently support the original WiFi to WiFi and BLE to BLE communications among multiple WiFi and BLE devices. ECT [33] proposed a network layer design for WiFi and ZigBee coexisted networks for reducing packet delivery delay in IoT networks.

In summary, algorithms have been proposed to solve the spectrum crisis problems. However, most of the work

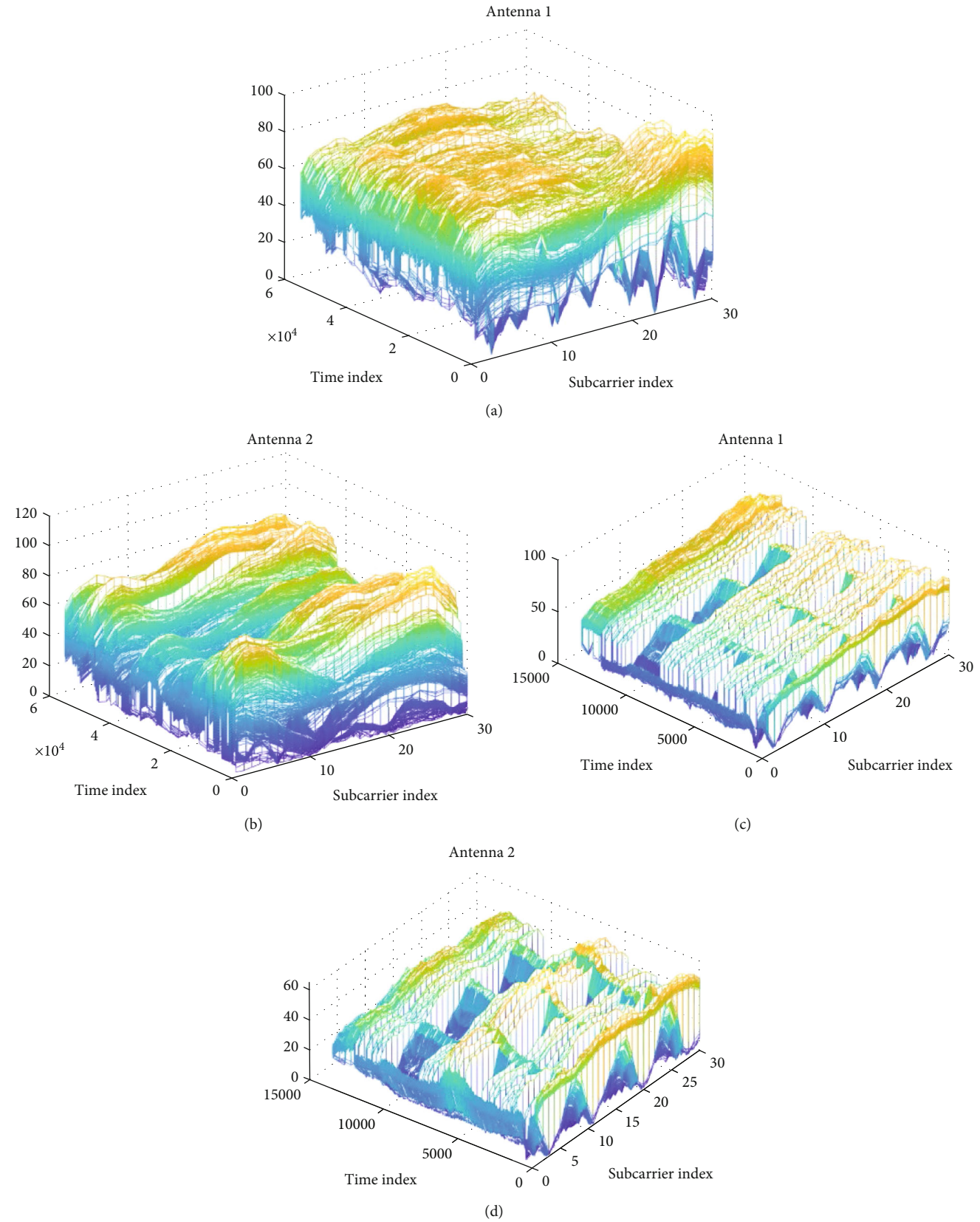

Figure 3: Examples of using CSI to sense subcarrier-level interference: (a) SNRs of antenna 1 calculated by CSI without interference; (b) SNRs of antenna 2 calculated by CSI without interference; (c) SNRs of antenna 1 calculated by CSI with three ZigBee interferences; (d) SNRs of antenna 2 calculated by CSI with three ZigBee interferences.

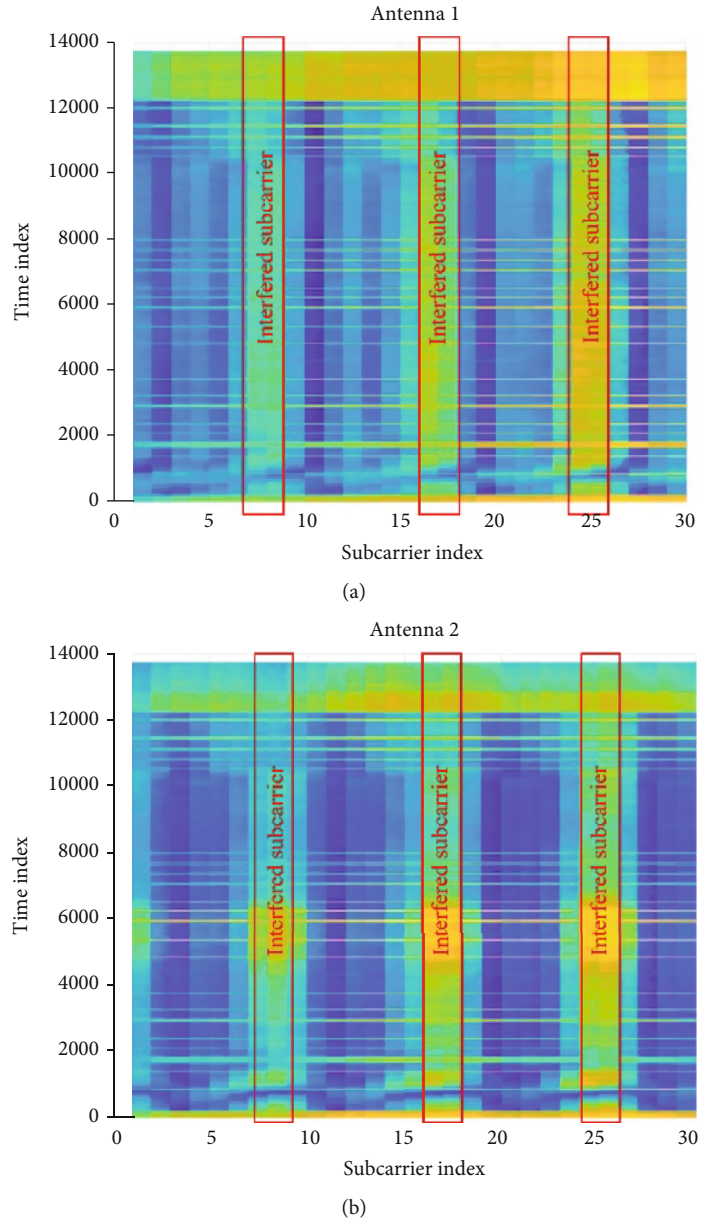

Figure 4: The difference between noninterfered subcarriers and interfered subcarriers: (a) data collected from antenna 1 and (b) data collected from antenna 2.

introduces additional monitoring systems or is not compatible with current IoT protocols. In this paper, we propose Subcarrier-Sniffier, which could utilize the off-the-shelf devices and network measurements to enable subcarrier-level spectrum sensing among the narrow-wide band or wide-wide band spectrum sharing scenarios.

3. Design of Subcarrier-Sniffer

According to the design challenges and our solutions, *Subcarrier-Sniffer* contains three parts: (i) channel state information collection and analysis module, (ii) CSI initial states establish and denoising module, and (iii) interfered range of target subcarrier determination module. The design overview of *Subcarrier-Sniffer* and the data stream among the three are shown in Figure 2.

The main functions of the three modules are shown as follows:

(1) *Channel State Information Collection and Analysis Module (Module 1)*. This module is responsible for collecting the channel measurements from off-the-shelf wideband wireless devices, such as the device that runs WiFi or LTE technologies. Currently, the important measurements of wireless technologies such as WiFi, ZigBee, and BLE are RSS (received signal strength) and CSI (channel state information), in which CSI is a complex number that describes the

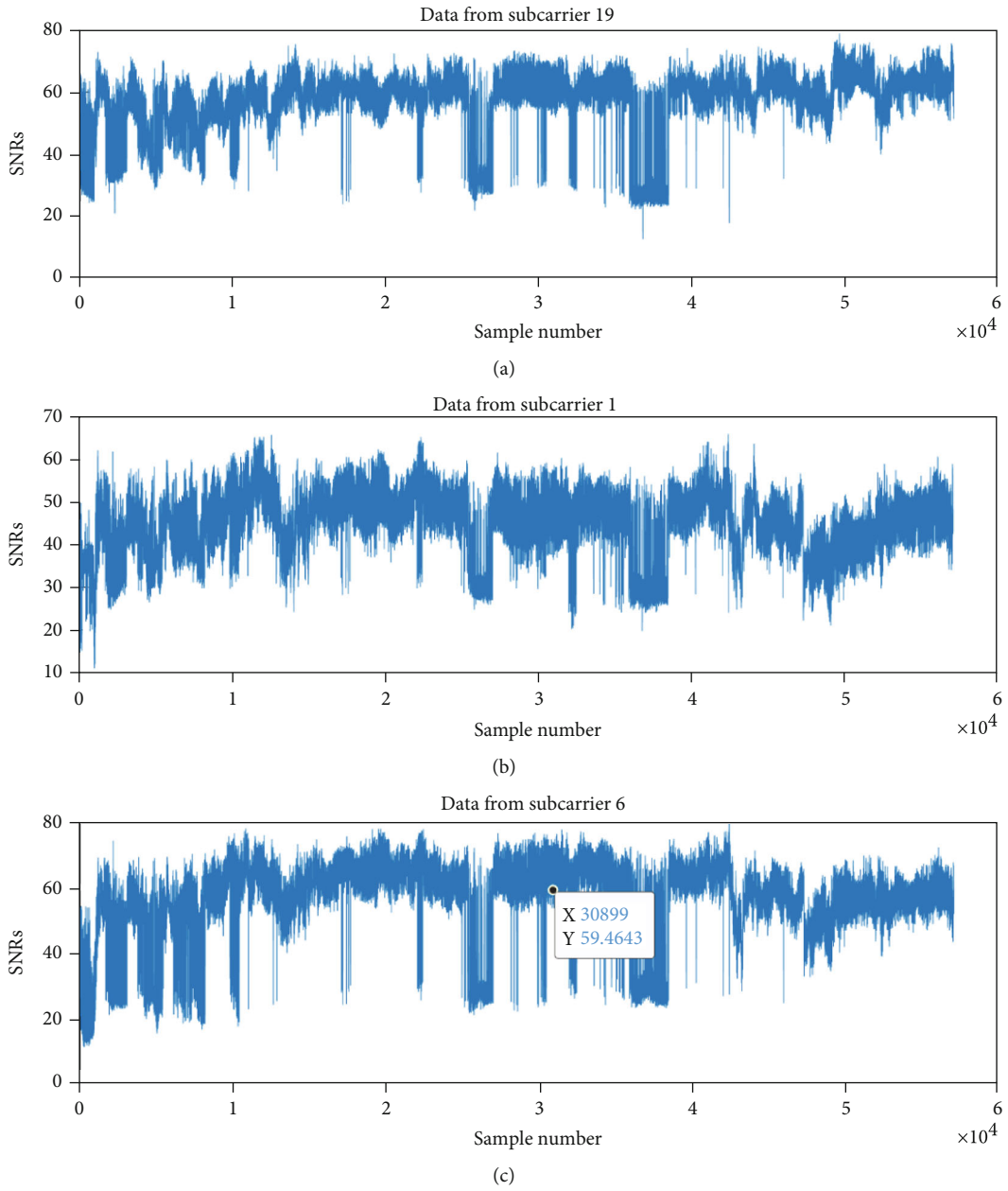

Figure 5: The variations of different subcarriers without any interference: (a) data from subcarrier 1; (b) data from subcarrier 6; (c) data from subcarrier 19.

phase and amplitude shift of arriving signals. The main procedures are detailed in Section 4 (1).

(2) *CSI Initial States Establish and Denoising Module (Module 2)*. This module is used for the initial CSI database establish by estimating noise caused by frequency selection characteristic when signal propagating in the indoor environments without any narrowband or wideband interference. The initial CSI database could provide a foundation to accurately fetch the pure subcarrier-level interference in normal communication links. The theory and procedures are detailed in Section 4 (2).

(3) Interfered range of target subcarriers determination module (module 3). This module is used to determine the range of interfered subcarriers according to the features of wireless measurements. The threshold-based methods were proposed to evaluate the interfered subcarriers more accurately. The procedures of this module are detailed in Section 4 (3).

3.1. Channel State Information Collection and Analysis Module. Channel state information collection and analysis module is to analyze the signal-to-noise ratios (SNRs) of the received signal for each subcarrier. The method is to

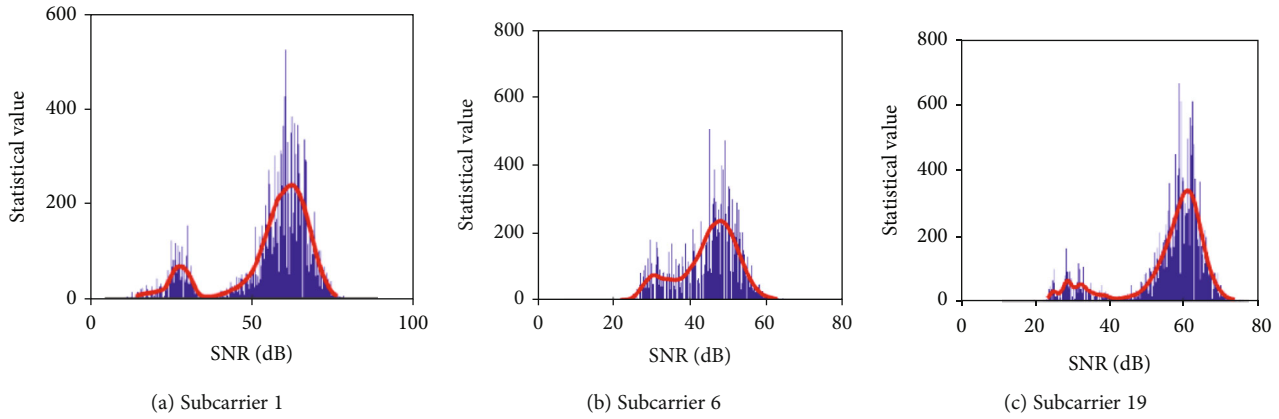

FIGURE 6: The initial state variations belong to different subcarriers: (a) the variations of subcarrier 1; (b) the variations of subcarrier 6; (c) the variations of subcarrier 19.

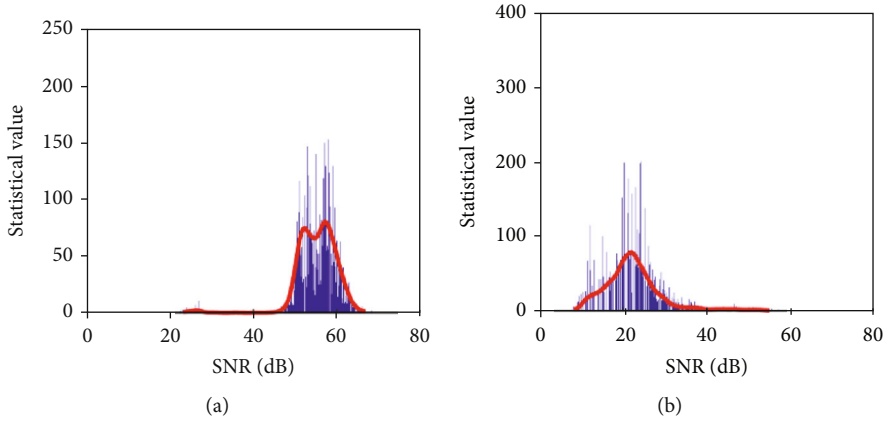

FIGURE 7: The initial state variations collected from different scenarios: (a) data from subcarrier 19 in indoor deployment and (b) data from subcarrier 19 in the outdoor deployment.

collect the CSI measurements to get the detailed information of each subcarrier, and the data structure of CSI received at a time t is shown in Equation (1) [14].

$$\text{CSI matrix}(t) = \begin{bmatrix} \text{csi}_{1,1}^t & \text{csi}_{1,2}^t & \cdots & \text{csi}_{1,m}^t \\ \text{csi}_{2,1}^t & \text{csi}_{2,2}^t & \cdots & \text{csi}_{2,m}^t \\ \text{csi}_{3,1}^t & \text{csi}_{3,2}^t & \cdots & \text{csi}_{3,m}^t \end{bmatrix}, \quad (1)$$

where each element in the matrix represents the j^{th} subcarrier from i^{th} communication link and each element in the CSI matrix is a complex number shown in Equation (2) [14].

$$\text{csi}_{i,j}^t = a + jb. \quad (2)$$

Therefore, at the time t, the signal-to-noise ratio (SNR) of j^{th}, the subcarrier of i^{th} communication link, can be calculated by Equation (3) [14].

$$\text{SNR}_{i,j}^t = \sqrt{a^2 + b^2}. \quad (3)$$

In order to verify that the CSI measurement could detect subcarrier-level SNRs, this paper uses Intel 5300 CSI acquisition tool to get CSI samples from wideband technology with interference from narrowband technology (ZigBee), and the experimental results are shown in Figure 3. The results show that the SNRs of the interfered subcarriers are different from those without any interference. Therefore, we propose to use CSI features to locate the interfered subcarriers when multiple devices content the same channel. The experimental results are analyzed from data via https://github.com/p01aris/csi_subcarrier_sniffer.

To observe the differences between interfered subcarriers and noninterfered clearly, Figure 4 is the two-dimension colormap of Figures 3(c) and 3(d). The interfered subcarriers are indicated by red rectangles showed in Figure 4, in which Figure 4(a) shows the data collected from antenna 1 while Figure 4(b) shows the data from antenna 2.

3.2. CSI Initial States Establish and Denoising Module. The experimental results in Figure 3 also show that the signal-to-noise ratios (SNRs) of different subcarriers also vary greatly without interference. The variations are different with different frequencies of each subcarrier. Figure 5(a) shows the variation of SNR series in subcarrier 1, while Figure 5(b)

shows the variation of SNR series in subcarrier 6, and Figure 5(c) shows the variation of SNRs series in subcarrier 19.

In summary, Figure 4 shows that the variations of SNRs of different subcarriers are various since the frequency selection features. Therefore, it is important to perceive the initial state of each subcarrier. The initial subcarrier states are also affected by the propagation environments.

Figure 5 shows the different variations without any interference from subcarrier 1, subcarrier 6, and subcarrier 19, respectively. The experimental results show that the variations belong to different subcarriers are various.

Figure 6 shows the statics value from subcarrier 1, subcarrier 6, and subcarrier 19, respectively, and the results further proved that the variations from different subcarriers are various without interference.

Figure 7 shows the statistical results of subcarrier 19 in indoor and outdoor deployment scenarios, respectively.

In summary, sensing the real-time initial state of each subcarrier is essential, and the specific procedures to fetch and store the initial CSI status are shown in Figure 2. If the RSS is in a normal state, recording the status of CSI as the initial state, the main reason is RSS seeks the average value of the received energy of the entire channel which could represent whether there is existing interference in the whole channel. Normally, when the jitter range of the RSS does not exceed 3 dB, it can be judged that there is no interference in the current time.

3.3. Interfered Range of Target Subcarrier Determination Module. Due to the existence of harmonic energy, the interference reflected from wideband technologies is wider than the narrowband interference. Figure 8 shows the practical interference caused by narrowband technology.

Figure 9 also shows the narrowband interference which is overlapped on the wideband signals. Therefore, the interference range determination process is significant to accurately locate the subcarrier-level interference when multiple heterogeneous wireless technologies coexist in the same deployment scenarios.

Figures 8 and 9 show that the energy generated by the harmonic portion also affects the wideband signal. Therefore, the subcarriers with harmonics also need to be considered as interfered subcarriers. To range the interfered subcarriers, the jitter value due to the interference should be calculated firstly by Equation (4).

$$\Delta \mathrm{snr}_{i,j}^{\tau} = \mathrm{SNR}_{i,j}^{\tau} - \mathrm{SNR}_{i,j}^{h}. \tag{4}$$

Suppose $\mathrm{flag}_{i,j}^{\tau}$ indicates whether subcarrier j on communication link i interferes at τ the time, $\mathrm{flag}_{i,j}^{\tau} = 0$ indicates that the subcarrier does not interfere, and $\mathrm{flag}_{i,j}^{\tau} = 1$ indicates that the subcarrier i interferes. The calculation method $\mathrm{flag}_{i,j}^{\tau}$ is as shown in Equation (5).

$$\mathrm{flag}_{i,j}^{\tau} = \begin{cases} 0\left(\left|\Delta \mathrm{snr}_{i,j}^{\tau}\right| < \varepsilon\right), \\ 1\left(\left|\Delta \mathrm{snr}_{i,j}^{\tau}\right| < \varepsilon\right), \end{cases} \tag{5}$$

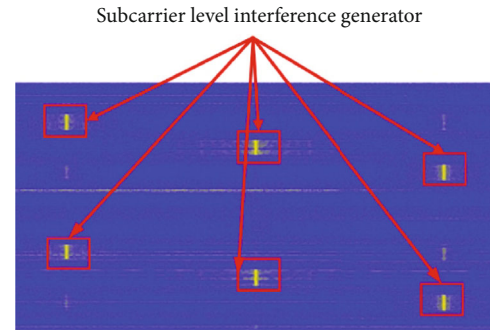

Figure 8: Interference of energy generated by harmonics on other subcarriers.

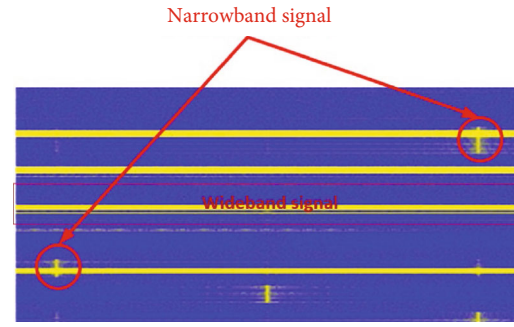

Figure 9: Interference caused by narrowband signals.

where ε is a threshold for determining whether subcarrier j on communication link i interfered. This value can be derived from the historical data of the communication error rate based on different values of ε. The experience value is around 6-10 dB.

4. Implementation and Experimental Results

This section implements the *Subcarrier-Sniffer* system and verified the experimental results according to the model in Section 4, we evaluated the performance of *Subcarrier-Sniffer* under different settings.

4.1. Implementation. The *Subcarrier-Sniffer* system contains three parts: (i) the wideband system transmitting and receiving end, the narrowband interfered signal generators, and the going-on signal monitor end. The configurations of the transmitting and receiving end of the wideband signals are shown in Table 1. The narrowband interfered signals are generated by USRP B200min. The going-on signal monitor end is implemented by USRP B200 and GNU radio platforms, and the structure of the monitor end is shown in Figure 10. The monitor end is to evaluate the performance of our proposed method, and the receiving end also could perform the monitoring function by using CSI value to judge the subcarrier-level interference in practical applications.

4.2. Experimental Results. To verify the performance of *Subcarrier-Sniffer*, this section evaluates the accuracy of the subcarrier-level spectrum sensing algorithm with the

Table 1: Wideband signal transmission and receiver configurations.

	Computer model	Network card model	Operating system	CSI tool	Other instructions
Sending end	DELL latitude E6440	AR9580	Ubuntu 14.04	Atheros CSI tool	Turn off the NIC back-off function
Receiving end	ThinkPad E40	AR9462	Ubuntu 14.04	Atheros CSI tool	Turn off the NIC back-off function

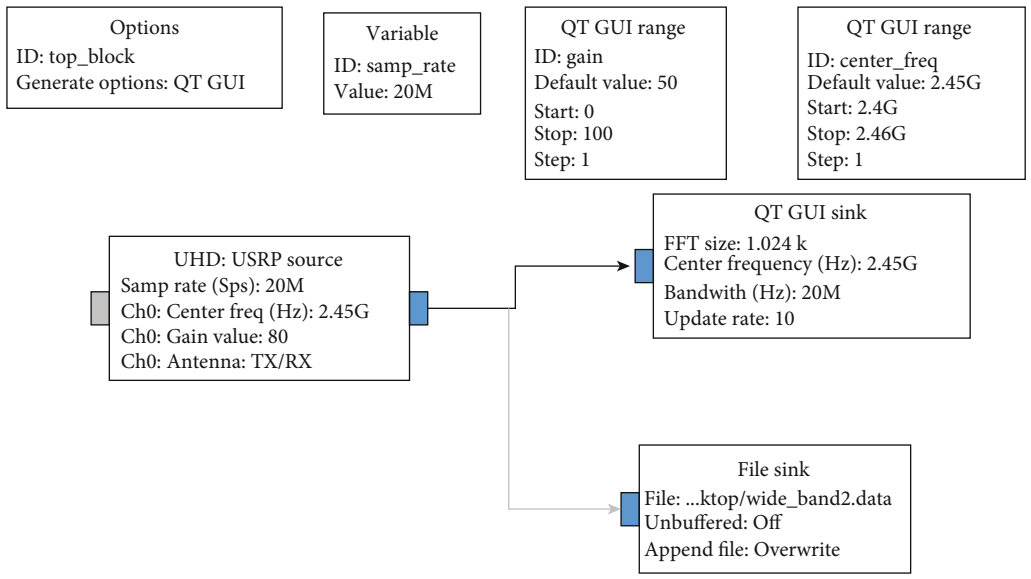

Figure 10: Implementation going-on signal monitor based on GNU radio.

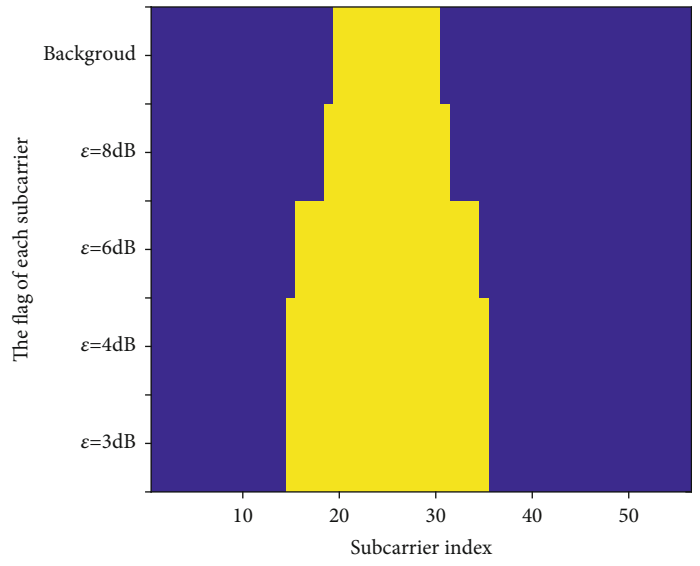

Figure 11: Subcarrier-level interference sensing results with the changes of ε.

changing of parameter ε, and the settings in this experiment are as follows: $dw = 7$m (the distance between wideband sender and wideband receiver) and di = 7m (the distance between narrowband interference generator and the wideband receiver). The sensing accuracies are shown in Figure 11, the bandwidth of the narrowband interference generator is 10 subcarriers, and the background is detailed in Table 2. The interference range determined by Subcarrier-Sniffer increases when ε is getting small, and trends are getting stable when $\varepsilon \leq 4$dB.

In order to further evaluate the performance of *Subcarrier-Sniffer*, we evaluate the sensing accuracy with the parameter di (the distance between narrowband interference generator and the wideband receiver); in this experiment, we assume $\varepsilon = 6$dB, and the results are shown in Table 3.

Table 2: Subcarrier interference sensing results in changes with ε.

Scenarios with different parameters	Interfered subcarriers
Background	[-5 -4 -3 -2 -1 1 2 3 4 5]
Subcarrier-Sniffer (ε = 8dB)	[-6 -5 -4 -3 -2 -1 1 2 3 4 5 6]
Subcarrier-Sniffer (ε = 6dB)	[-8 -7 -6 -5 -4 -3 -2 -1 1 2 3 4 5 6 7 8]
Subcarrier-Sniffer (ε = 4dB)	[-9 -8 -7 -6 -5 -4 -3 -2 -1 1 2 3 4 5 6 7 8 9]
Subcarrier-Sniffer (ε = 3dB)	[-9 -8 -7 -6 -5 -4 -3 -2 -1 1 2 3 4 5 6 7 8 9]

Table 3: The situation of subcarrier interference sensing result changes with di.

Scenarios	Interfered subcarrier
Background (ε = 6dB)	[-5 -4 -3 -2 -1 1 2 3 4 5]
Subcarrier-Sniffer (di = 0.5m)	[-12 -11 -10 -9 -8 -7 -6 -5 -4 -3 -2 -1 1 2 3 4 5 6 7 8 9 10 11 12]
Subcarrier-Sniffer (di = 2.5m)	[-10 -9 -8 -7 -6 -5 -4 -3 -2 -1 1 2 3 4 5 6 7 8 9 10]
Subcarrier-Sniffer (di = 5m)	[-8 -7 -6 -5 -4 -3 -2 -1 1 2 3 4 5 6 7 8]
Subcarrier-Sniffer (di = 10m)	[-5 -4 -3 -2 -1 1 2 3 4 5]
Subcarrier-Sniffer (di = 12.5m)	[null]

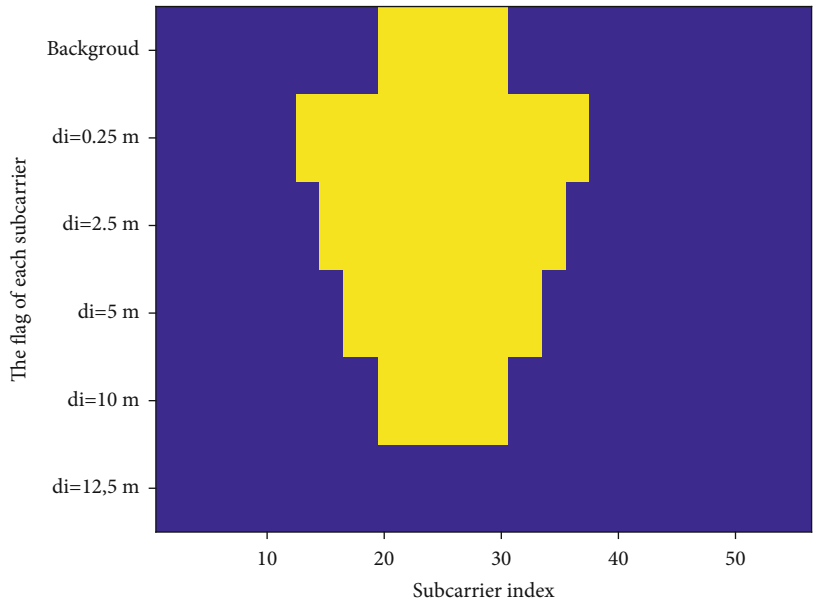

Figure 12: Subcarrier-level interference sensing results with the changes of di.

The results in Table 3 show that the interference determination range is larger when di is smaller (detailed in Figure 12); the reason is when di is smaller, the harmonic energy generated by the narrowband signal is relatively higher. When di ≥ 12.5m, the number of interfered subcarriers sensed by *Subcarrier-Sniffer* is 0. The main reason is the interference generator is far from the signal receiver, and it could not interfere with the received signals.

5. Conclusion

To further optimize the spectrum utilization of the ISM band, this paper proposes *Subcarrier-Sniffer*, a subcarrier-level spectrum sensing algorithm. *Subcarrier-Sniffer* contains three parts: (i) channel state information collection and analysis module, (ii) CSI initial states establish and denoising module, and (iii) interfered range of target subcarrier determination module. Compared with traditional channel-

based spectrum sensing algorithms, subcarrier-level spectrum sensing algorithms could further improve the ISM spectrum utilization. The experimental results show that the sensing accuracies of *Subcarrier-Sniffer* are changing with ε and di, where ε is the threshold to decide when the subcarrier is interfered with by other technologies and di is the distance between narrowband interference generator and the wideband receiver.

Subcarrier-Sniffer could be widely used in cross-technology coexisting environment, and we will introduce *Subcarrier-Sniffer* to WiFi and ZigBee and WiFi and LTE coexisting wireless networks to increase the spectrum utilization in our future works; WiFi and ZigBee coexisting work should be an example for any wideband and narrowband coexisting scenarios, while WiFi and LTE coexisting work should be an example solution for wideband and wideband coexisting scenarios; more precise fine-grained spectrum sensing and sharing methods are also our future concerns to further optimize the spectrum utilization in ISM bands.

Data Availability

The data that support the findings of this study are openly available in csi_subcarrier_sniffer at https://github.com/p01aris/, reference number Bsg-c000083.

Conflicts of Interest

The authors declare that they have no conflicts of interest.

Acknowledgments

This project is supported by the CERNET Innovation Project (NGII20180315), Undergraduate Training Programs for Innovation and Entrepreneurship Project of Jilin Province (2020JLSFDX-JSJ03 and 2020JLSFDX-JSJ05), and Science and Technology Project of Jilin Provincial Department of Education (JJKH20210457KJ). We also thank anonymous reviewers and their valuable comments.

References

[1] T. Barnett, S. Jain, U. Andra, and T. Khurana, *Cisco visual networking index (VNI) global mobile data traffic, 2017-2022*, Americas/EMEAR Cisco Knowledge Network (CKN) Presentation, 2018.

[2] K. Davaslioglu, S. Soltani, T. Erpek, and Y. E. Sagduyu, "DeepWiFi: cognitive WiFi with deep learning," *IEEE Transactions on Mobile Computing*, vol. 20, no. 2, pp. 429–444, 2021.

[3] Y. Zhu, L. Liu, J. Li, J. Yu, and C. Long, "OutSense: out-of-band sensing with ZigBee sensors for channel adaptation in wireless LANs," in *Proceedings of the International Conference on Parallel and Distributed Systems*, pp. 92–99, Melbourne, VIC, Australia, 2015.

[4] X. Zhang, Y. Zhang, Y. Ma, and Y. Gao, "RealSense: real-time compressive spectrum sensing testbed over TV white space," in *IEEE 18th International Symposium on A World of Wireless, Mobile and Multimedia Networks (WoWMoM)*, pp. 1–3, Macau, 2017.

[5] M. Hirzallah, W. Afifi, and M. Krunz, "Full-duplex spectrum sensing and fairness mechanisms for Wi-Fi/LTE-U coexistence," in *IEEE Global Communications Conference*, pp. 1–6, Washington, DC, 2016.

[6] E. Pei, X. Lu, B. Deng, J. Pei, and Z. Zhang, "The impact of imperfect Spectrum sensing on the performance of LTE licensed assisted access scheme," *IEEE Transactions on Communications*, vol. 68, no. 3, pp. 1966–1978, 2020.

[7] C. Cano, D. J. Leith, A. Garcia-Saavedra, and P. Serrano, "Fair coexistence of scheduled and random access wireless networks: unlicensed LTE/WiFi," *IEEE/ACM Transactions on Networking*, vol. 25, no. 6, pp. 3267–3281, 2017.

[8] P. Gawlowicz, A. Zubow, and A. Wolisz, "Enabling cross-technology communication between LTE unlicensed and WiFi," in *IEEE Conference on Computer Communications*, pp. 144–152, Honolulu, HI, 2018.

[9] D. Saliba, R. Imad, S. Houcke, and B. E. Hassan, "WiFi dimensioning to offload LTE in 5G networks," in *IEEE 9th Annual Computing and Communication Workshop and Conference*, pp. 0521–0526, Las Vegas, NV, USA, 2019.

[10] Y. Gao, Z. Qin, Z. Feng, Q. Zhang, O. Holland, and M. Dohler, "Scalable and reliable IoT enabled by dynamic spectrum management for M2M in LTE-A," *IEEE Internet of Things Journal*, vol. 3, no. 6, pp. 1135–1145, 2016.

[11] H. Sun, Z. Fang, Q. Liu, Z. Lu, and T. Zhu, "Enabling LTE and WiFi coexist in 5GHz for efficient spectrum utilization," *Journal of Computer Networks and Communications*, vol. 2017, Article ID 5156164, 17 pages, 2017.

[12] F. Li, J. Luo, G. Shi, and Y. He, "ART: adaptive frequency-temporal co-existing of ZigBee and WiFi," *IEEE Transactions on Mobile Computing*, vol. 16, no. 3, pp. 662–674, 2017.

[13] F. Chiti, R. Fantacci, F. Nizzi, L. Pierucci, and T. Pecorella, "A cooperative spectrum sensing protocol for IEEE 802.15.4m wide-area WSNs," in *IEEE International Conference on Communications*, pp. 1–6, Paris, 2017.

[14] Z. Chi, Y. Li, H. Sun, Y. Yao, Z. Lu, and T. Zhu, "B2W2: N-way concurrent communication for IoT devices," in *14th ACM Conference on Embedded Network Sensor Systems*, pp. 245–258, New York, NY, USA, 2016.

[15] Z. Chi, Y. Li, Z. Huang, H. Sun, and T. Zhu, "Simultaneous bidirectional communications and data forwarding using a single ZigBee data stream," in *IEEE Conference on Computer Communications*, pp. 577–585, Paris, France, 2019.

[16] S. Pan, X. Zhao, and Y. C. Liang, "Robust power allocation for OFDM-based cognitive radio networks: a switched affine based control approach," *IEEE Access*, vol. 5, pp. 18778–18792, 2017.

[17] H. Zhang, L. L. Yang, and L. Hanzo, "Compressed sensing improves the performance of subcarrier index-modulation-assisted OFDM," *IEEE Access*, vol. 4, pp. 7859–7873, 2016.

[18] T. Agrawal, V. Lakkundi, A. Griffin, and P. Tsakalides, "Compressed sensing for OFDM UWB systems," in *IEEE Radio and Wireless Symposium*, pp. 190–193, Phoenix, AZ, USA, 2011.

[19] A. Razavi, M. Valkama, and D. Cabric, "Compressive identification of active OFDM subcarriers in presence of timing offset," in *IEEE Global Communications Conference*, pp. 1–6, San Diego, CA, USA, 2015.

[20] Y. Zeng, S. W. Oh, and R. Mo, "Subcarrier sensing for distributed OFDMA in powerline communication," in *IEEE International Conference on Communications*, pp. 1–5, Dresden, Germany, 2009.

[21] W. Xu, W. Xiang, M. Elkashlan, and H. Mehrpouyan, "Spectrum sensing of OFDM signals in the presence of carrier frequency offset," *IEEE Transactions on Vehicular Technology*, vol. 65, no. 8, pp. 6798–6803, 2016.

[22] H. Sun, Z. Fang, X. Liu, and Z. Lu, "Insightful causes and potential resolutions for spectrum crisis in ISM bands: a survey," *The Journal of Communication*, vol. 11, no. 9, pp. 862–870, 2016.

[23] J. Fang, K. Tan, Y. Zhang et al., "Fine-grained channel access in wireless LAN," *IEEE/ACM Transactions on Networking*, vol. 21, no. 3, pp. 772–787, 2013.

[24] S. Han, X. Zhang, and K. G. Shin, "Fair and efficient coexistence of heterogeneous channel widths in next-generation wireless LANs," *IEEE Transactions on Mobile Computing*, vol. 15, no. 11, pp. 2749–2761, 2016.

[25] S. Yun, D. Kim, and L. Qiu, "Fine-grained spectrum adaptation in WiFi networks," in *Proceedings of the 19th Annual International Conference on Mobile Computing & Networking*, pp. 327–338, New York, NY, USA, 2013.

[26] Y. Xiao, "IEEE 802.11n: enhancements for higher throughput in wireless LANs," *IEEE Wireless Communications*, vol. 12, no. 6, pp. 82–91, 2005.

[27] IEEE, "802.11ac," https://standards.ieee.org/standard/802_11ac-2013.html.

[28] S. Rayanchu, V. Shrivastava, S. Banerjee, and R. Chandra, "Fluid: improving throughputs in enterprise wireless LANs through flexible channelization," *IEEE Transactions on Mobile Computing*, vol. 11, no. 9, pp. 1455–1469, 2012.

[29] F. Wu, N. Singh, N. Vaidya, and G. Chen, "On adaptive-width channel allocation in non-cooperative, multi-radio wireless networks," in *Proceedings IEEE INFOCOM*, pp. 2804–2812, Shanghai, China, 2011.

[30] R. Chandra, R. Mahajan, T. Moscibroda, R. Raghavendra, and P. Bahl, "A case for adapting channel width in wireless networks," *ACM SIGCOMM Computer Communication Review*, vol. 38, no. 4, pp. 135–146, 2008.

[31] A. Hussain and N. A. Saqib, "Effects of adaptable channelization in Wi-Fi networks," in *11th International Conference on Innovations in Information Technology*, pp. 166–171, Dubai, United Arab Emirates, 2015.

[32] T. Moscibroda, R. Chandra, Y. Wu, S. Sengupta, P. Bahl, and Y. Yuan, "Load-aware spectrum distribution in wireless LANs," in *IEEE International Conference on Network Protocols*, pp. 137–146, Orlando, FL, USA, 2018.

[33] H. Rahul, N. Kushman, D. Katabi, C. Sodini, and F. Edalat, "Learning to share: narrowband-friendly wideband networks," in *Proceedings of the ACM SIGCOMM 2008 conference on Data communication*, pp. 147–158, New York, NY, USA.